Reference frame continuity under the effects of great earthquakes

Demián Gómez[1,2], Diego Piñón[2,3], Robert Smalley[1], Michael Bevis[4], Sergio Cimbaro[2], Luis Lenzano[5], Jorge Barón[5]

1.Center for Earthquake Research and Information, The University of Memphis, 2.Dirección de Geodesia, Instituto Geográfico Nacional Argentino, 3. Space Research Centre, Royal Melbourne Institute of Technology
4.School of Earth Sciences, Ohio State University, 5.Universidad Nacional de Cuyo, Argentina.

Abstract: Several recent great earthquakes have produced regional to continental sized non-secular post-seismic deformation fields that are easily resolvable with GPS, requiring further development of geodetic reference frame velocities to include these effects. The 2010, (Mw 8.8) Maule, Chile, earthquake produced a measurable, non-secular, post-seismic signal within latitudes 28°S to 40°S extending from the Pacific to the Atlantic. Using continuous GPS (CGPS) data from the Red Argentina de Monitoreo Satelital Continuo and Central Andes GPS Project, we fit an extended trajectory model (ETM) including secular South American plate velocity and boundary deformation, co-seismic discontinuity, and a non-secular, logarithmic post-seismic transient produced by the earthquake in the Posiciones Geodésicas Argentinas 2007 (POSGAR07) reference frame. We used least squares collocation (LSC) to model both the background secular inter-seismic and the non-secular post-seismic components of the ETM to predict movement of passive geodetic benchmarks where continuous monitoring is not available. We tested the LSC model using campaign and CGPS data not used to generate the model and found standard deviations (95% confidence level) for the north and east components of 3.8 mm and 5.5 mm, respectively, indicating that the model predicts the post-seismic deformation field very well. Finally, we added a co-seismic displacement field, estimated using an elastic finite element model. The final, trajectory prediction model ties the post-earthquake coordinates to POSGAR07 within 5 cm for ~91% of the passive test benchmarks

Introduction

Bevis and Brown (2014) present an extended trajectory model (ETM) and demonstrate that its application to reference frame (RF) materialization can considerably reduce systematic errors in RF realization. In addition to the secular velocities used in constant velocity models (CVM), their ETM contains static offsets to model equipment changes and co-seismic jumps, sinusoidal components to model observed cyclic displacements, and logarithmic transients to model non-secular after slip and visco-elastic relaxation. The mathematical expression for the ETM is:

$$\mathbf{x}(t) = \sum_{i=1}^{n_p+1} \mathbf{p}_i (t-t_R)^{i-1} + \sum_{j=1}^{n_j+1} \mathbf{b}_j H(t-t_j) + \sum_{k=1}^{n_F} \mathbf{s}_k \sin(w_k t) + \mathbf{c}_k \cos(w_k t) + \sum_{i=1}^{n_T} \mathbf{a}_i \log[1+(t-t_{EQ})/T_i]$$

Methodology

To describe the CGPS trajectories we used $n_p = 1$, since none of the time series display observable pre-seismic accelerations. Two frequencies, annual and semi-annual, are typically sufficient to model the observed cyclic behavior and we used $n_F = 2$ for these components. Finally, for the logarithmic post-seismic transients from the 2010 Maule earthquake, we applied a value of $T = 0.5$ years for the relaxation time of all the CGPS time series. This is different from the value $T = 1$ year proposed by Bevis and Brown (2014). In general, the logarithmic transient adjustment is relatively insensitive to the exact value of T, and we found that using $T = 0.5$ allowed us to use single relaxation time for the whole network while providing a good fit for both the near and far field post-seismic time series. Figure 1 shows an example of the ETM adjustment of RAMSAC station MZAC located in the near field of the Maule earthquake (Mendoza, Argentina)

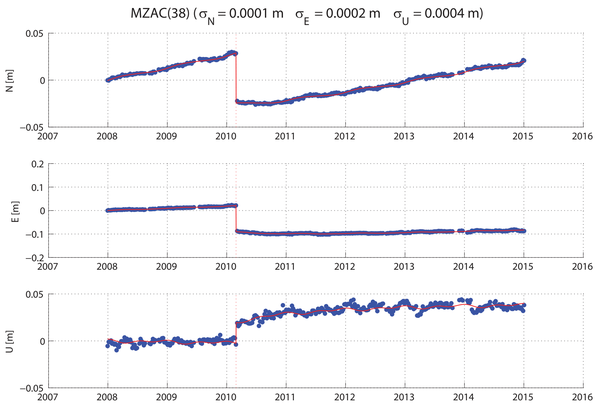

Figure 1: ETM of RAMSAC station MZAC. Co-, post- and inter-seismic components can be observed. The vertical component also shows a cyclic signal. The north and east components also have cyclic components that are not visible due to the scale of the co-seismic displacement.

The ETM provides an estimation of the inter-seismic velocities, which were interpolated using LSC to obtain the secular velocity field. To apply LSC we first remove plate motions using the ITRF compatible, no-net-rotation (NNR), Actual Plate Kinematic Model (APKIM, Drewes, 2009). Figure 2 shows the result of this interpolation procedure. We called this velocity model the "linear Argentine Velocity" model (*Velocidades Argentinas Lineales*, Vel-Ar-Lin)

[1] Bevis, M., and A. Brown 2014. Trajectory models and reference frames for crustal motion geodesy. Journal of Geodesy, 88(3), 283–311.
[2] Drewes, H., O. Heidbach (2012). The 2009 Horizontal Velocity Field for South America and the Caribbean. In: Kenyon S., M.C. Pacino, U. Marti (Eds.), "Geodesy for Planet Earth", IAG Symposia, 136: 657-664.
[3] Kearsley, W. (1977), Non-stationary estimation in gravity prediction problem. Report 256, Department of Geodetic Science, The Ohio State University, Columbus
[4] Ligas, M., Kulczycki, M., (2010) Simple spatial prediction - least squares prediction, simple kriging, and conditional expectation of normal vector, Geodesy and Cartography. Volume 59, Issue 2, Pages 69–81, DOI: 10.2478/v10277-012-0002-0
[5] Moritz, H. (1978), Least-squares collocation, Rev. Geophys., 16(3), 421–430, doi:10.1029/RG016i003p00421.
[6] Moritz H (1980) Advanced physical geodesy. Abacus, Tunbridge Wells
[7] Sevilla, M. L. (1987), Colocación por mínimos cuadrados, IV Curso de Geodesia Superior, Instituto de Astronomía y Geodesia, Madrid.
[8] Vieira, S., et al., (2009) Detrending non stationary data for geostatistical applications. Bragantia, Campinas v. 69, Suplemento, 1-8.
[9] Tong, X., et al. (2010), The 2010 Maule, Chile earthquake: Downdip rupture limit revealed by space geodesy, Geophys. Res. Lett., 37, L24311, doi:10.1029/2010GL045805.

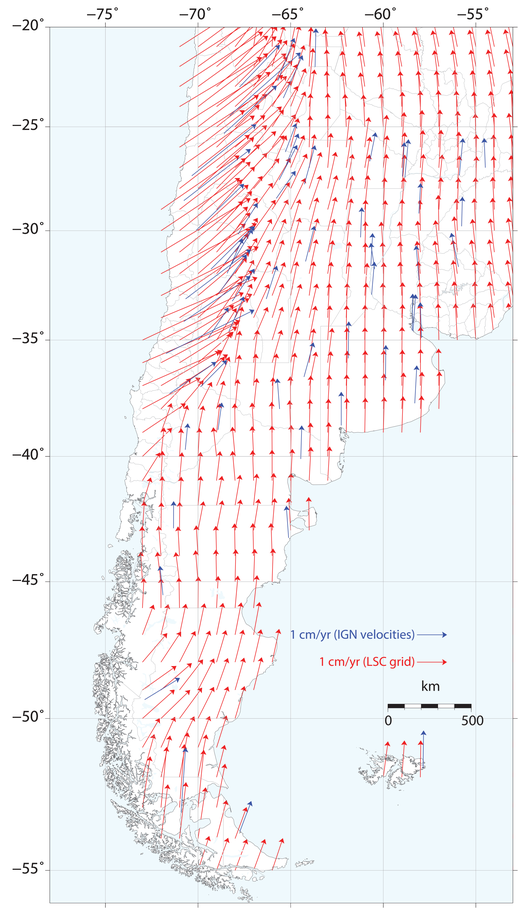

Figure 2: Least squares collocation of the secular inter-seismic velocities of the RAMSAC, CAP and IGS networks in POSGAR07 RF. Blue arrows show the CGPS stations used for the interpolation. Red arrows show the 1 by 1 degree grid of interpolated velocities.

We then studied the post-seismic transient field estimated from the ETM. We detrended the non-secular transients produced by the 2010 Maule earthquake using a spatial exponential taper. The stable sills observed in the semi-variograms show that the non-secular velocities can be modeled as a stationary process (Figure 3).

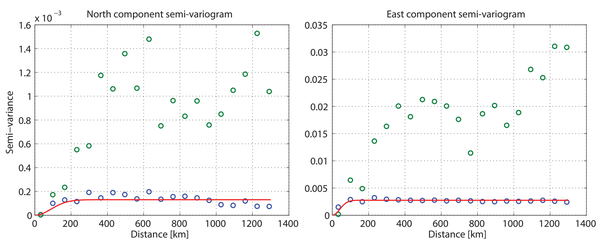

Figure 3: Semi-variogram plots of the north and east components of the post-seismic transient after applying an exponential taper detrending function. Blue circles show the detrended data, green circles show the original data, and the solid line is the Gaussian semi-variance model.

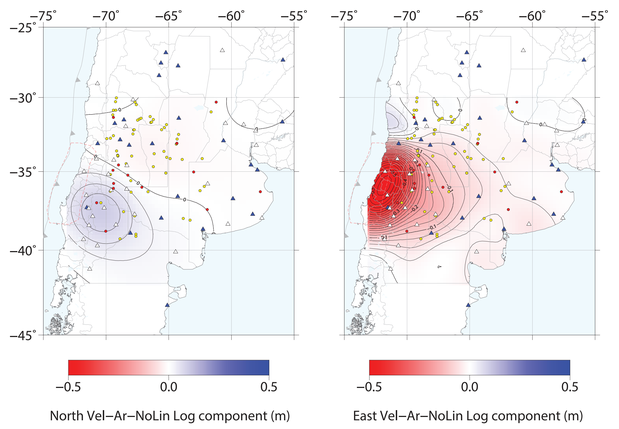

Figure 4: Least squares collocation model of the logarithmic transients. Blue triangles show the CGPS stations that have ~2 or more years of pre-earthquake data. White triangles show CGPS that don't meet the condition to be included in the Vel-Ar-Lin estimation. Red circles show the test stations, which have multiple measurements, used to verify the quality of the Vel-Ar-Lin and Vel-Ar-NoLin models. Yellow circles are POSGAR benchmarks with only one measurement before and one after the earthquake. Contours of logarithmic transients every 0.025 m. Red dashed line shows the 2010 Maule earthquake rupture zone as defined by aftershocks.

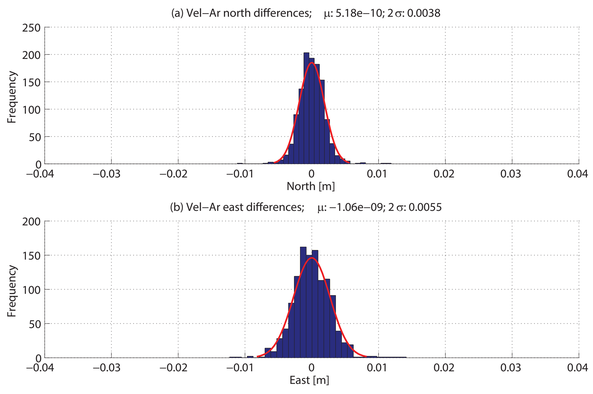

Figure 5: Histogram of model minus observation frequency and fit to normal distribution for (a) north and (b) east components, for CAP and RAMSAC CGPS sites and CAP campaign sites with multiple measurements used in the test. We note a slight tendency towards negative values. This tendency reveals the presence of a small systematic bias, probably due to the misfit of the logarithmic transient observed during the first month after the earthquake. Bevis and Brown (2012) showed that this misfit can be reduced by adjusting the value of the relaxation time for each time series. For the precision and purposes of the model developed here, however, these misfits are negligible.

Least squares collocation of the logarithmic transients

Figure 4 shows the result of the LSC of the non-secular velocity component of the CGPS sites. We called this model "Argentine Non-Linear Velocities" (*Velocidades Argentinas No Lineales*, Vel-Ar-NoLin). Using Vel-Ar-NoLin and the data not included in the LSC (Figure 4, red circles), we calculated the trajectory of CAP campaign and CGPS sites to validate Vel-Ar-NoLin. Using the misfits obtained from the model validation, we plotted the histograms on Figure 5. We found that Vel-Ar-NoLin accurately describes the non-secular velocity field produced by the Maule earthquake.

Results and conclusions

To successfully tie the pre- and post-seismic states of the RF, we used a finite element model (FEM) of the co-seismic displacements. By adding the co-seismic displacement model to the secular and non-secular LSC models (Vel-Ar-Lin and Vel-Ar-NoLin), we obtain a trajectory prediction model (TPM), Argentine Velocities (*Velocidades Argentinas*, Vel-Ar). We tested the ability of the TPM to tie the pre- and post-seismic states of POSGAR07 using the POSGAR sites that were not used in the calculation of Vel-Ar (Figure 4, yellow filled circles). We compared the predicted post-seismic coordinate to the post-seismic measurement. The misfits in the north and east components are shown in Figure 6, where we note that 38 of 60 sites (~63%) fall inside the 2.5 cm limit, 17 (~28%) fall between 2.5 and 5 cm, and 5 (~8%) fall outside the 5 cm limit. Only one measurement falls outside the 10 cm limit (with a misfit of 13.8 cm), although we do not discard the possibility of a blunder in the measurement or processing of that site.

This methodology can be used to update VEMOS by incorporating a logarithmic transient LSC model and a co-seismic displacement model. Updating VEMOS in this manner would allow it to predict the velocities of the SIRGAS RF in a non-linear-model (modelos no lineales, MoNoLin), without having to break the model into multiple, sequential, linear segments as proposed by Drewes and Sánchez (2014).

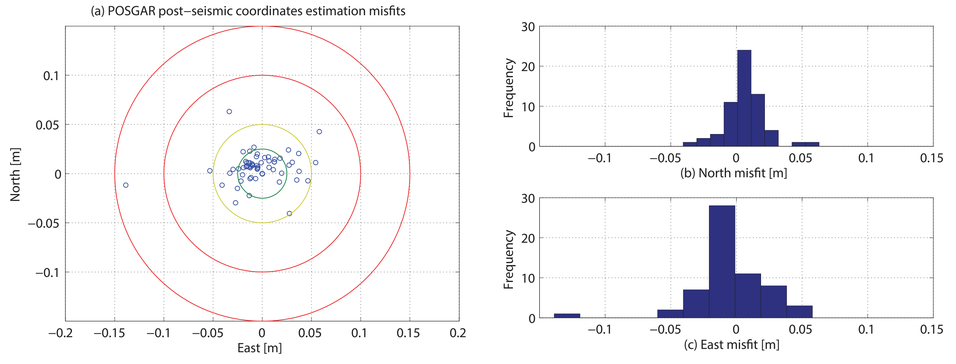

Figure 6: Misfit between the post-seismic measurements of POSGAR benchmarks. Green, yellow and red circles represent a misfit distance of 2.5 cm, 5 cm, 10 and 15 cm. Test sites are shown in Figure 4 by yellow filled circles. (b) Histogram of north component differences. (c) Histogram of east component differences.

Acknowledgements and data sources

We thank Hernán Guagni, Agustín Raffo and the Department of Geodesy of the IGN for providing the GPS processing and additional support. We also thank Benjamin Brooks and James Foster for providing additional GPS data used in this work and Wolfgang Schwanghart for providing his semi-variogram code through the Matlab File Exchange. This work was supported by the NSF Collaborative Research: Great Earthquakes, Megathrust Phenomenology and Continental Dynamics in the Southern Andes, award number EAR-1118241, and the Center for Earthquake Research and Information, University of Memphis. Additional publicly available time series of CGPS stations located in Chile (and that are not part of CPC-Ar) were obtained from the Nevada Geodetic Laboratory: http://geodesy.unr.edu/